Daniel Geisler, Joseph A. King, Klaas Bahnsen, Fabio Bernardoni, Arne Doose, Dirk K. Müller, Michael Marxen, Veit Roessner, Martijn van den Heuvel, Stefan Ehrlich

Altered White Matter Connectivity in Young Acutely Underweight Patients With Anorexia Nervosa

Erstveröffentlichung in / First published in:

Journal of the American Academy of Child and Adolescent Psychiatry : JAACAP. 2022, 61 (2), S. 331 - 340. {Zugriff am: 24.02.2023}. Elsevier. ISSN 1527-5418.

DOI: https://doi.org/10.1016/j.jaac.2021.04.019

Final edited form was published in "Journal of the American Academy of Child and Adolescent Psychiatry : JAACAP". 61 (2), S. 331 - 340. ISSN 1527-5418.
https://doi.org/10.1016/j.jaac.2021.04.019

Altered White Matter Connectivity in Young Acutely Underweight Patients With Anorexia Nervosa

Daniel Geisler, MSc, Joseph A. King, PhD, Klaas Bahnsen, BSc, Fabio Bernardoni, PhD, Arne Doose, MSc, Dirk K. Müller, MSc, Michael Marxen, PhD, Veit Roessner, MD, Martijn van den Heuvel, PhD, Stefan Ehrlich, MD, PhD

Objective: Reductions of gray matter volume and cortical thickness in anorexia nervosa (AN) are well documented. However, findings regarding the integrity of white matter (WM) as studied via diffusion weighted imaging (DWI) are remarkably heterogeneous, and WM connectivity has been examined only in small samples using a limited number of regions of interest. The present study investigated whole brain WM connectivity for the first time in a large sample of acutely underweight patients with AN.

Method: DWI data from predominantly adolescent patients with acute AN (n = 96, mean age = 16.3 years) and age matched healthy control participants (n = 96, mean age = 17.2 years) were analyzed. WM connectivity networks were generated from fiber tractography derived streamlines connecting 233 cortical/subcortical regions. To identify group differences, network based statistic was used while taking head motion, WM, and ventricular volume into account.

Results: Patients with AN were characterized by 6 WM subnetworks with abnormal architecture, as indicated by increased fractional anisotropy located primarily in parietal occipital regions and accompanied by reduced radial diffusivity. Group differences based on number of streamlines reached only nominal significance.

Conclusion: Our study reveals pronounced alterations in the WM connectome in young patients with AN. In contrast to known reductions in gray matter in the acutely underweight state of AN, this pattern does not necessarily indicate a deterioration of the WM network. Future studies using advanced MRI sequences will have to clarify interrelations with axonal packing or myelination, and whether the changes should be considered a consequence of undernutrition or a vulnerability for developing or maintaining AN.

Key words: anorexia nervosa, structural connectivity, white matter, diffusion weighted imaging, fiber tractography

Anorexia nervosa (AN) is a severe eating disorder that typically begins during adolescence and is characterized by an intense preoccupation with body image, fear of weight gain, energy intake restriction, and severe emaciation. Several well-powered structural magnetic resonance imaging studies have established widespread atrophic changes in cortical gray matter (GM) as well as white matter (WM) volume reductions in acutely underweight patients with AN (acAN).[1,2] Studies going beyond measures of WM volume by using diffusion weighted imaging (DWI) have reported less consistent results.[3] Microstructural WM aberrations in AN have been identified particularly in cingulum and corpus callosum but also in other regions including thalamo-cortical and occipital parietal temporal frontal tracts.[4–7] The results are partially heterogeneous with respect to either localization or directionality of the observed changes, which may be attributed to the methodology used, partial volume effects, or modest and/or heterogeneous sample sizes.[5]

The majority of previous studies targeting WM microstructure in AN have used standard methods comparing diffusion strength on the voxel level or tract level (tract-based spatial statistics [TBSS]). A more elaborate method of fiber tractography takes not only the magnitude but also the direction of diffusion tensors into account. This technique thus enables quantification of structural connectivity of WM between brain regions.[8] To date, only 6 known studies have applied fiber tractography in acAN or long-term weight-recovered AN (recAN) samples, and all were limited by their focus on specific tracts or connectivity from a few predetermined seed regions.[9–14]

Advances in brain network analyses allow examination of whole-brain connectivity by combining fiber tractography

Final edited form was published in "Journal of the American Academy of Child and Adolescent Psychiatry : JAACAP". 61 (2), S. 331 - 340. ISSN 1527-5418.
https://doi.org/10.1016/j.jaac.2021.04.019

and graph-theoretic techniques modelling the brain's architecture as a complex network.[15] Graph theory designates the brain as a set of nodes (representing brain areas or voxels across the whole brain) connected by edges (interregional structural connections).[15]

To determine differences in WM network architecture between female acAN patients and pairwise age-matched healthy control participants (HC), we applied a hypothesis-free approach that uses whole-brain parcellation to model a graph-theoretic network. Then we carried out network-based statistic (NBS)[16] to identify deviant connectivity patterns (subnetworks). Previous studies have used NBS to identify altered WM network topology in patients with several different disorders,[17,18] but this is its first application in AN.

METHOD

Participants

After excluding outliers and applying an automated pairwise age-matching strategy (for details, see Supplement 1, available online; age difference between matched pairs ranging between 0 and 2.2 years, with a mean of 0.9 years), we analyzed data from 96 adolescents or young adult female acAN patients (age range 12.1 28.9 years, with 8 participants >21 years) and 96 female healthy control participants (age range 12.1 28.6 years, with 8 participants >21 years). AcAN patients were recruited from specialized eating disorder programs at child and adolescent psychiatry and psychosomatic departments of a university hospital, and underwent magnetic resonance imaging (MRI) within 96 hours after beginning behaviorally oriented nutritional rehabilitation programs. All participants were examined using the expert version of the Structured Interview for Anorexia and Bulimia Nervosa for *DSM-IV* (SIAB-EX), supplemented by our own semi-structured research interview. AcAN patients had to have a body mass index (BMI) below the 10th age percentile (if <16 years of age) or a BMI <17.5 kg/m^2 (if >16 years of age) and no recent weight gain.

The HC participants were recruited through advertisements among middle school, high school, and university students. To be included in the HC group, participants had to be of normal weight and eumenorrheic. HC participants were excluded if they had any history of psychiatric illness, a lifetime BMI below the 10th age percentile if <18 years of age, or a BMI <18.5 kg/m^2 if >18 years of age, or were currently obese (BMI over the 92th age percentile if <18 years of age; BMI over 29 kg/m^2 if >18 years).

Participants of both study groups were excluded if they had a lifetime history of any of the following clinical diagnoses: organic brain syndrome, schizophrenia, substance dependence, psychosis number of streamlines (NOS), bipolar disorder, bulimia nervosa, or binge-eating disorder (or "regular" binge eating, defined as bingeing at least once a week for 3 or more consecutive months). Further exclusion criteria were psychotropic medications within 4 weeks prior to the study, substance abuse or any medical condition that might affect appetite, eating behavior, or body weight.

This study was approved by the local Institutional Ethics Review Board, and all participants (and their guardians if underage) gave written informed consent. For further details regarding the sample and clinical measures, see Supplement 1, available online.

Clinical Measures

Eating disorder specific psychopathology of all participants was assessed with the German version of the Eating Disorders Inventory (EDI-2). Depressive symptoms were explored using the German version of the Beck Depression Inventory (BDI-2). Supplement 1, available online, provides more details on the assessment instruments.

MRI Data Acquisition

Images were acquired between 8 and 9 am after an overnight fast on a 3T MRI scanner (TRIO; Siemens, Erlangen, Germany) using a 12-channel head coil.

High-resolution 3D T1-weighted structural scans were acquired using a rapid acquisition gradient echo (MP-RAGE) sequence with the following parameters: voxel size = 1.0×1.0×1.0 mm^3, field of view (FoV) = 256×224×176 mm^3, 176 sagittal slices, no inter-slice gap, TE = 2.26 milliseconds, TR = 1.9 seconds, flip angle = 9°, bandwidth of 200 Hz/pixel, and prescan normalize. Diffusion-weighted imaging data were collected using a spin-echo sequence at 2.4 mm isotropic voxel resolution, 307×307×144 mm^3 FoV, 128×128 matrix size, 60 slices, no inter-slice gap, TE = 104 milliseconds, TR = 15 seconds, BW = 2056 Hz/Px, GRAPPA acceleration factor 2, 24 reference lines, and prescan normalize. A total of 32 diffusion sensitizing gradients (b = 1,300 s/mm^2) were applied, and 4 images without diffusion weighting (b = 0 s/mm^2) were acquired.

MRI Data Pre-processing

Structural MRI. The data were analyzed in an automated manner with FreeSurfer (http://surfer.nmr.mgh.harvard.edu, version 5.1.0), a software package for cortical surface reconstruction and volumetric segmentation.

The brain of each participant was parcellated/segmented into 233 regions of interest (ROIs; 219 cortical and 14 subcortical) on the basis of a high-resolution subdivision of FreeSurfer's Desikan-Killiany atlas.[19] The standard output of FreeSurfer also includes total volume of

Final edited form was published in "Journal of the American Academy of Child and Adolescent Psychiatry : JAACAP". 61 (2), S. 331 - 340. ISSN 1527-5418.
https://doi.org/10.1016/j.jaac.2021.04.019

WM, volumes of left/right lateral ventricles, volume of the third ventricle, and intracranial volume, which were later used as nuisance covariates in the analysis of DWI data to account for potential differences in WM volumes and partial volume effects due to ventricular enlargement in acAN patients.[20,21] Further details regarding the pre-processing of the data and the atlas are provided in Supplement 1, available online.

Diffusion Weighted MRI. The DWI pre-processing pipeline has been described in detail previously,[22] and involved the following steps: (1) diffusion-weighted data were realigned, corrected for Eddy current induced distortions and participant movements using Eddy from FSL (https://fsl.fmrib.ox.ac.uk). The output of the estimated frame-wise motion parameter was averaged across volumes and later used as nuisance variable. (2) We fitted a diffusion profile within each voxel using 32 weighted images and the average $b = 0$ image from each participant. From the resulting tensor, the main diffusion direction in each voxel was computed as the principal eigenvector resulting from the eigenvalue decomposition of the fitted tensor, marking the preferred diffusion direction in each voxel. For each voxel, the fractional anisotropy (FA), mean diffusivity (MD), radial diffusivity (RD), and axial diffusivity (AD) were computed (see Supplement 1, available online).

Fibertracking. Using the extracted information on the preferred diffusion direction within each voxel in the brain mask, the WM tracts of the whole brain network were reconstructed using the deterministic fiber tracking,[22] based on the fiber assignment by continuous tracking (FACT) algorithm.[23] Fibers were reconstructed by starting 8 seeds in each voxel and following the main diffusion direction of each voxel (selected as the principal eigenvector) until 1 of the following stopping criteria was reached: the fiber tract (1) entered a voxel with a low level of diffusion preference (FA <0.1), (2) made an unexpected sharp angular turn (angle $>45°$), or (3) left the brain mask.

Network Construction. The network consisted of the 233 ROIs, also called nodes, which are pairwise connected by edges associated with weights. For every edge, we determined those fibers crossing the 2 given ROIs. The NOS of an edge is the count of fibers associated with the edge. The FA, MD, RD, and AD value of an edge is the respective weighted mean of all voxels crossed by the fiber segments connecting the ROIs.[22,24] The network construction resulted in 5 symmetric 233×233 connectivity matrices for each participant.

Quality Control. For each participant, we defined connections as those with NOS ≥ 3; otherwise the edge was marked as nonexistent, and its weight was set as a missing value in all of the participant's connectivity matrices. Then we calculated the average connectivity by averaging the connectivity matrices, resulting in mean values for NOS, FA, MD, RD, and AD for each participant.

The prevalence of an edge is the percentage of this edge existing in its reference group (acAN or HC). The participant's prevalence of existing edges is the average prevalence value of all edges that are existent. Similarly, we calculated the participant's prevalence of nonexisting edges.

By applying the Carling criterion for outlier detection, a participant was marked as an outlier and excluded if (1) a participant's average connectivity value was an outlier in the reference group, or (2) the average frame-wise motion (taken from Eddy output) was an outlier in its reference group, or (3) the prevalence of existing or non-existent edges was an outlier in its reference group. Then the final connectivity matrices were thresholded such that only edges with a prevalence of $>60\%$ across all participants were included.[25] Supplement 1, available online, provides details on outlier removal, prevalence threshold, age-matching, and partial sample overlap with a previous DWI study from our laboratory.

Group Comparison of Demographic and Clinical Variables

Group differences were tested using Student t tests. The statistical assumption were checked using a combination of statistical tests and visual inspection of the histograms. Because of the possible violation of normality specifically in the HC group, we applied the nonparametric Mann–Whitney U test for the group comparison of the BDI-2 total score.

Network-Based Statistic

Network-based statistic (NBS) is a powerful statistical method for identifying a statistically significant cluster of connections indicating differences between groups (t test or a more general statistical model) on intermediate network scales.[16]

As described in our previous functional studies,[26,27] NBS is computed using the following steps: (1) identify all connections (pairs of nodes) that are different between groups beyond a particular t value (called primary threshold); (2) select the largest contiguous cluster of these connections; and (3) validate the cluster's significance by permutation testing. In permutation testing, an empirical null distribution of the largest cluster size is generated by conducting the first 2 NBS steps on resampled group membership data 10,000 times. The returned subnetwork is statistically significant at a family-wise error (FWE) corrected value of $p < 0.05$.

Final edited form was published in "Journal of the American Academy of Child and Adolescent Psychiatry : JAACAP". 61 (2), S. 331 - 340. ISSN 1527-5418.
https://doi.org/10.1016/j.jaac.2021.04.019

Although the network needs to be considered as a whole, the extent of the returned network can be varied using a different primary threshold. This adjusts the extremity of deviation in a connection between groups required, before it is considered for inclusion in the NBS result. The NBS returns a single p value that represents the likelihood that the subnetwork (also called component) is due to a true effect in the data. This approach measures the entire cluster of returned connections but does not identify the contribution of each connection independently, and thus does not allow for the interpretation of single connections.

To account for possible influencing effects due to motion or potential WM volume reduction in acAN, we used a regression model in which, in addition to group, the variables WM volume, motion, and the interaction of group and WM volume were included (see Supplement 1, available online). These predictor variables were also included in all follow-up statistical analyses.

The NBS procedure was carried out for NOS and FA matrices, and for the contrasts acAN<HC and acAN>HC, with a primary threshold of $t = 3.1$ (which corresponds to $p = .001$). Because of the 4-fold comparison, we report only components with a Bonferroni-adjusted p value (nominal p value $\times$ 4; denoted by p_{comp}) of <.05 (which corresponds to an adjusted significance level of 0.0125).

To ensure that our results were not biased, we conducted a number of subanalyses that are summarized here and described in detail in Supplement 1, available online. The included subanalyses address the following: (A) effects of age, by restricting the matched sample to participants <18 years of age and covarying for age, (B) effects of IQ by covarying for IQ, (C) effects of current comorbid psychiatric diagnosis by excluding patients with comorbidities, (D) partial volumes effects[21] by (D1) covarying for ventricular volumes, (D2) an alternative approach of covarying for ventricular volumes (using principal components), as well as (D3) a method correcting for free water,[28] and (E) possibility of spurious (non-anatomical) connections by restricting the analysis to connection with ≥10 fibers.

Relationship to Clinical Variables

The connectivity values for components with significant group differences were calculated for each participant by averaging the participant's weights of all edges included in a given component. To test associations with clinical variables in acAN, robust linear models were fitted (see Supplement 1, available online). The severity of eating disorder symptoms (EDI-2 core) served as the main predictor variable, but the effects of possibly confounding variables such as depression (BDI-2 total score), age-adjusted BMI standard deviation scores (BMI-SDS; see Supplement 1, available online), and urine specific gravity (USG) were also explored. USG can help to understand whether results are influenced by hypo- or hyperhydration, which may be more prevalent in acAN.[5] Akin to the group comparisons, all regression models also included age, WM volume, and motion as nuisance variables.

From the estimated models, we extracted the standardized regression coefficients of the clinical variables and estimated the p values using Wald tests. We adjusted the p values (denoted by p_{adj}) for the number of components, using the Benjamini Hochberg procedure.

RESULTS

Sample Characteristics

As expected, there were no group differences in age. BMI was drastically reduced, and eating disorder symptoms and depressive symptoms (and also IQ) were increased in acAN (Table 1, and also see Tables S1 and S2, available online).

Group Differences in FA Networks

When comparing FA networks between groups, we found 6 distinct components with increased FA in acAN (Figure 1A, Table 2). The largest components, CFA1 and CFA2, were located in frontolateral parietal regions of the right and left hemisphere, respectively (19 edges with p_{comp}< .0001 each). The components CFA3 and CFA4 were found in predominately parietal occipital areas of the left and right hemisphere (11 and 8 edges with p_{comp}= .0004). The edges of CFA5 mostly comprised regions of the right cingulate and precuneus (7 edges with p_{comp}= .0004). The smallest component, CFA6, encompassed 4 edges connecting divisions of the right temporal lobe and right insula (p_{comp}= .008). There were no significant components in the contrast HC>acAN. A follow up analysis indicated that the increase of FA associated with the 6 components was driven by a marked reduction in RD values of the connections, whereas AD was mostly unaffected except in CFA3 (see Table S3, available online).

A number of subanalysis (A E; see Methods) were conducted to ensure that our results were not biased by (A) age effects, (B) differences in IQ between groups, (C) effects of current comorbid psychiatric diagnosis, (D) partial volume effects, or (E) spurious connections. In all of these analyses, the results were highly comparable to those in our main analysis (see Tables S4 S10 and Figure S1, available online).

Group Differences in Networks Based on NOS

The group comparison of NOS networks resulted in 3 distinct but relatively small components (3 edges with p_{comp}= .01 each) of decreased NOS in acAN (Figure 1B, Table 3). The left-hemispheric components CNOS1 and

Final edited form was published in "Journal of the American Academy of Child and Adolescent Psychiatry : JAACAP". 61 (2), S. 331 - 340. ISSN 1527-5418.
https://doi.org/10.1016/j.jaac.2021.04.019

TABLE 1 Basic Demographic and Clinical Variables

	HC (n = 96)		acAN (n = 96)				
	Mean	**SD**	**Mean**	**SD**	**Statistic**	***p***	***d***
Age (y)	17.2	3.3	16.3	3.3	1.9	.0617	0.3
BMI (kg/m^2)	20.7	2.0	14.7	1.4	23.7	.0000	3.4***
BMI SDS	−0.1	0.6	−3.1	1.3	21.0	.0000	3.0***
IQ	109.3	9.5	115.3	11.7	−3.8	.0002	−0.6***
EDI 2 core score	47.3	15.7	77.8	20.6	−11.3	.0000	−1.7***
BDI 2 total score	5.3	5.4	22.6	10.9	−607.5	.0000	−2.0***
Motion (mm)	0.2	0.1	0.2	0.1	−0.3	.7280	−0.1
Average NOS per edge	75.4	8.3	72.5	8.8	2.4	.0188	0.3*
Average FA per edge	0.38	0.02	0.40	0.02	−6.9	.0000	−1.0***
White matter volume (cm^3)	429.6	42.1	419.4	40.0	1.7	.0862	0.2
Urine specific gravity	—	—	1.010	0.003	—	—	—

Note: Averages of number of streamlines (NOS) and fractional anisotropy (FA) are calculated by averaging the connectivity matrix of each participant. Motion was calculated by averaging the frame wise motion estimates from Eddy correction across volumes. Group differences were tested using Student t tests (and in the case of the BDI 2, a Mann Whitney U test to meet assumptions). In all, 95% of the patients acutely underweight with AN (acAN) were predominately of the restrictive subtype, and 5% were predominately of the binge/purge subtype, as ascertained with the SIAB EX interview. In the acAN group, 15% of the patients had 1 or more associated current psychiatric comorbidities (7% depressive disorders, 4% obsessive compulsive disorders, 4% anxiety disorders, 2% tic Tourette, 1% adaptation disorder, 1% personality disorders, and 1% developmental disorders; for details on assessment, see Supplement 1, available online). Please refer to Table S1 (duration of illness and the Eating Disorders Inventory [EDI 2] total score) and Table S2, available online (detailed information from a subset of SIAB EX item scores), available online. BDI 2 Beck depression inventory 2, BMI body mass index, BMI SDS age adjusted BMI standard deviation scores, HC healthy control participants, WM white matter.
**p < .05; *** p < .001.*

CNOS2 connect regions in the cuneus and regions in the pre- and postcentral areas, respectively. CNOS3 was located in the right occipital and temporal areas. We did not find any components of increased NOS in acAN. When taking partial volume effects into account, no significant components were present (subanalysis D2). Most of the other subanalyses also found no differences between acAN and HC except for CNOS1 (A, C, D1, and E), CNOS2 (B and E), and CNOS3 (E). The results of the subanalyses A E are summarized in Tables S11 S15 and Table S16, available online.

Relationship to Clinical Variables in the acAN Group

We did not find evidence for a relationships between eating disorder symptoms (EDI-2 core score) and any of the component (all $|\beta| \leq 0.23$, $p_{adj} \geq .093$). BMI-SDS was negatively associated with component CFA3 ($\beta = 0.33$, $p_{adj} = .036$; all remaining components $|\beta| \leq 0.23$, $p_{adj} \geq .251$).

There were no significant relationships between the components and depression symptoms (BDI-2 total score) or urine specific gravity (all $|\beta| \leq 0.133$, $p_{adj} \geq .750$).

DISCUSSION

In a comparatively large sample of young acAN patients and pairwise age-matched HC, we found aberrations of the WM network architecture in the patient group using a graph-theoretical approach. The network structure in acAN was characterized by 6 components with abnormally increased FA in WM tracts transversing several regions in the frontal, parietal, and occipital lobes. We also found 3 smaller components of reduced indices of connectivity (based on NOS) in the patient group. However, in contrast to the FA-based components, only the first NOS component was confirmed in some of the subanalyses, but no NOS components were present when correcting for free water. This suggests that the altered NOS connectivity in patients might be largely attributable to partial volume effects.

Although several previous DWI studies in various AN samples (using mostly traditional analysis methods comparing diffusion strength on the voxel level or on the tract level) often found decreased FA,[5-7] our findings of increased FA are more in line with 2 tractography-based studies,[10,11] and 2 traditional DWI studies in adolescents.[29,30] Our subanalyses suggest that the observed increase in FA in all 6 subnetworks may have been driven by a reduction in RD, which might, for example, indicate an increased density in axonal packing.[31] Interestingly, previous studies in the field of cognitive training have associated such patterns of diffusion parameters with increased efficiency of neural conduction (eg, Keller and Just[32]). This interpretation would be in line with the findings of a traditional TBSS study, which also found widespread increases in FA in young acAN patients.[30] The authors of the latter report speculated that dense axonal packing

Final edited form was published in "Journal of the American Academy of Child and Adolescent Psychiatry : JAACAP". 61 (2), S. 331 - 340. ISSN 1527-5418.
https://doi.org/10.1016/j.jaac.2021.04.019

FIGURE 1 Network-Based Statistic (NBS) Components

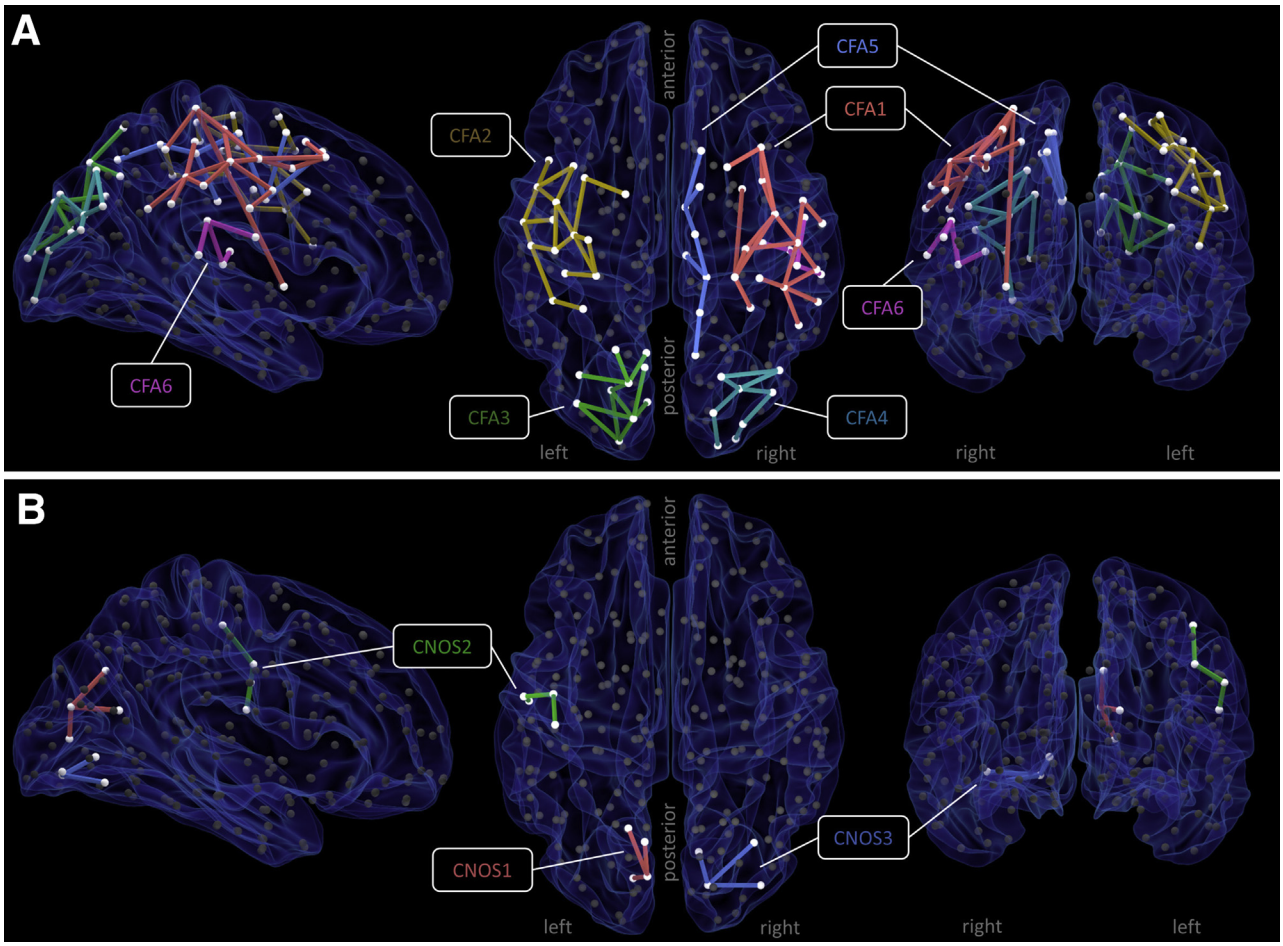

Note: Results of the NBS at the primary threshold of t = 3.1 are shown. Components are depicted as connected edges of the same color. (A) Group differences acAN>HC in FA weighted network (see Table 2 for details). (B) Group differences based on number of streamlines (see Table 3) only reached nominal significance or were not significant in a number of subanalyses (see Supplement 1, Tables S11 S15 and Table S16 for a summary, available online). Please note color figures are available online.

could be associated with premorbid factors, namely, pre-existing WM-fibers that exhibit more directionality due to less crossing fibers, or, alternatively, with starvation-related factors, namely, a decrease in surrounding tissue volume or an increase in the fiber diameter due to axonal swelling. Starvation-related effects have been shown to affect gray matter, in a relatively global way.[1] The relative lack of associations with BMI and the identification of specific and anatomically as well as functionally meaningful subnetworks (while controlling for total WM volumes and ventricular volumes as well as free water) characterized by increased FA, as shown in the current study, may be seen as evidence against purely starvation-related effects. However, several previous (classical) DWI studies have reported regionally reduced white matter microstructure,[5-7] and available longitudinal data of DWI studies in AN seem to point toward normalization of altered WM with weight recovery.[4,30] Furthermore, findings regarding GM volume alterations in AN are also suggestive of (partial) normalization during recovery.[33]

More specifically regarding the localization of the group differences revealed in our study, the right- and left-hemispheric frontolateral parietal components (CFA1 and CFA2) encompassed the caudal part of the middle frontal cortex, the superior frontal cortex, post- and pre-central areas, and the supramarginal gyrus. These regions are connected by the inferior fronto-occipital fasciculus and superior longitudinal fasciculus. These results converge with those from both classical as well as hypothesis-driven tractography studies that have reported alterations in AN in both of these WM tracts[10,13,14,29,34] (see Supplement 1, available online).

Altered functional magnetic resonance imaging (fMRI) activation in AN during performance of a target-

Final edited form was published in "Journal of the American Academy of Child and Adolescent Psychiatry : JAACAP". 61 (2), S. 331 - 340. ISSN 1527-5418.
https://doi.org/10.1016/j.jaac.2021.04.019

TABLE 2 Connections of Fractional Anisotropy (FA) Network-Based Statistic (NBS) Components

Component CFA1 – right frontolateral–parietal			*(p_{comp}<.0001)*
Right Putamen	– rh postcentral 5	rh supramarginal 1	– rh supramarginal 2
rh caudalmiddlefrontal 1	– rh caudalmiddlefrontal 3	rh supramarginal 1	– rh supramarginal 3
rh caudalmiddlefrontal 1	– rh precentral 4	rh postcentral 5	– rh precentral 4
rh postcentral 3	– rh precentral 3	rh postcentral 5	– rh precentral 5
rh postcentral 3	– rh precentral 4	rh postcentral 5	– rh superiorparietal 1
rh postcentral 3	– rh precentral 5	rh inferiorparietal 2	– rh supramarginal 1
rh postcentral 3	– rh supramarginal 1	rh postcentral 2	– rh precentral 3
rh postcentral 3	– rh supramarginal 3	rh precentral 4	– rh precentral 5
rh caudalmiddlefrontal 3	– rh precentral 4	rh postcentral 4	– rh supramarginal 1
rh caudalmiddlefrontal 3	– rh superiorfrontal 8		
Component CFA2 – left frontolateral–parietal			*(p_{comp}<.0001)*
lh caudalmiddlefrontal 2	– lh precentral 5	lh postcentral 5	– lh postcentral 6
lh caudalmiddlefrontal 2	– lh precentral 7	lh postcentral 5	– lh supramarginal 5
lh caudalmiddlefrontal 3	– lh precentral 4	lh postcentral 6	– lh precentral 6
lh caudalmiddlefrontal 3	– lh superiorfrontal 9	lh postcentral 6	– lh precentral 7
lh parsopercularis 2	– lh precentral 7	lh precentral 3	– lh precentral 4
lh postcentral 2	– lh postcentral 3	lh precentral 4	– lh precentral 5
lh postcentral 2	– lh precentral 3	lh postcentral 4	– lh postcentral 5
lh postcentral 2	– lh precentral 4	lh postcentral 4	– lh precentral 4
lh precentral 5	– lh precentral 7	lh postcentral 4	– lh precentral 5
lh superiorparietal 2	– lh supramarginal 5		
Component CFA3 – left parietal–occipital			*(p_{comp}=.0004)*
lh cuneus 1	– lh superiorparietal 7	lh precuneus 3	– lh superiorparietal 5
lh inferiorparietal 1	– lh lateraloccipital 1	lh precuneus 4	– lh superiorparietal 7
lh inferiorparietal 1	– lh superiorparietal 7	lh superiorparietal 4	– lh superiorparietal 5
lh inferiorparietal 4	– lh superiorparietal 5	lh superiorparietal 5	– lh superiorparietal 6
lh lateraloccipital 1	– lh superiorparietal 6	lh superiorparietal 6	– lh superiorparietal 7
lh lateraloccipital 1	– lh superiorparietal 7		
Component CFA4 – right parietal–occipital			*(p_{comp}= .0004)*
rh inferiorparietal 4	– rh superiorparietal 5	rh lateraloccipital 1	– rh superiorparietal 7
rh inferiorparietal 4	– rh superiorparietal 6	rh lateraloccipital 2	– rh lateraloccipital 3
rh inferiorparietal 6	– rh lateraloccipital 2	rh superiorparietal 5	– rh superiorparietal 6
rh inferiorparietal 6	– rh superiorparietal 6	rh superiorparietal 6	– rh superiorparietal 7
Component CFA5 – right cingulate–precuneus			*(p_{comp}= .0004)*
rh paracentral 2	– rh paracentral 3	rh posteriorcingulate 1	– rh superiorfrontal 5
rh paracentral 2	– rh posteriorcingulate 1	rh posteriorcingulate 1	– rh superiorfrontal 6
rh paracentral 3	– rh posteriorcingulate 2	rh precuneus 4	– rh precuneus 5
rh paracentral 3	– rh precuneus 5		
Component CFA6 – right temporal–insula			*(p_{comp}= .008)*
rh postcentral 1	– rh supramarginal 4	rh supramarginal 4	– rh transversetemporal 1
rh superiortemporal 1	– rh supramarginal 4	rh transversetemporal 1	– rh insula 1

Note: Components and their respective edges of the group comparison acAN>HC of the FA weighted networks at primary threshold of t 3.1. Edges are listed as pairs of ROIs. Also refer to Figure 1A. FA fractional anisotropy, lh left hemisphere, NBS network based statistic, rh right hemisphere.

Final edited form was published in "Journal of the American Academy of Child and Adolescent Psychiatry : JAACAP". 61 (2), S. 331 - 340. ISSN 1527-5418.
https://doi.org/10.1016/j.jaac.2021.04.019

TABLE 3 Connections of Number of Streamlines (NOS) Network-Based Statistic (NBS) Components

Component CNOS1 – left cuneus			*(p_{comp}=.01)*
lh cuneus 1	– lh pericalcarine 1	lh cuneus 1	– lh precuneus 5
lh cuneus 1	– lh precuneus 4		
Component CNOS2 – left pre postcentral			*(p_{comp}=.01)*
lh postcentral 4	– lh precentral 6	lh postcentral 6	– lh precentral 6
lh postcentral 6	– lh postcentral 7		
Component CNOS3 – right occipital–temporal			*(p_{comp}=.01)*
rh fusiform 1	– rh lingual 1	rh lingual 1	– rh lingual 2
rh lateraloccipital 4	– rh lingual 1		

Note: Components and their respective edges of the group comparison acAN<HC of the NOS weighted networks at primary threshold of t 3.1. Edges are listed as pairs of ROIs. Also refer to Figure 1B. lh left hemisphere, NBS network based statistic, rh right hemisphere.

involved (together with the superior parietal regions) in spatially guided behaviors and mental imagery.[38] Of note, the precuneus was shown to play a major role in disorders related to alterations of bodily awareness.[39] In a face- and house-matching task, patients with AN and patients with body dysmorphic disorder showed abnormal fMRI activation in the precuneus and lateral occipital cortex, which was suggested to be related to the distorted perceptions underlying appearance concerns in both disorders.[40] It is noteworthy that CFA3 was the only component in which FA correlated with BMI-SDS (negatively) in the acAN group (and, as a *post hoc* analysis revealed, also in HC: $\beta = \quad 0.31$, $p = .003$), and the only component with reduced AD (which has been associated with axonal damage). Although this correlation should be interpreted with caution and may merely be a consequence of the acutely underweight state in the patient group, low BMI may be a potential proxy for a hidden trait associated with more severe illness. Indeed, results from genetic studies suggest a negative genetic correlation between genes predisposing toward AN and risk genes for a larger BMI.[41]

The precuneus is also involved in right-hemispheric CFA5 that encompasses areas of the paracentral, superior frontal, and posterior cingulate cortices. Several of these midline structures are also involved in the integration of self-referential information.[42] The same brain regions are also recruited in monetary and social identity tasks that require participants to make self-referential decisions, during which both recAN and acAN seem to show abnormal neural responses.[43,44]

The smallest component, right-hemispheric CFA6, was located in the insula, supramarginal cortex, and temporal and postcentral cortices. A large body of literature has made connections among the insula, changes in interoceptive attention and awareness,[45] and AN. For example, aberrant functional connectivity of the insula during the resting state[26,46,47] and altered connectivity of the insula using seed-based tractography has been demonstrated for AN.[12,14] However, in a number of subanalyses, CFA6 did not include the insula as a node, which might be a consequence of the loss of power due to the inclusion of more covariates in the model.

The results of our study have to be considered within the following limitations: First, because the characteristics of diffusion depend on a broad range of factors (eg, axon diameter, packing density of fibers, membrane permeability, and myelination), the interpretation of DWI findings is challenging. Although decreased FA (and increased RD) is usually (but not always) associated with impaired fiber integrity, increased FA is not always associated with superior function or health.[30] Furthermore, inaccuracies of the tensor-fitting algorithm in particular in areas with crossing fibers also remain a challenge for all DWI studies and warrant a cautious interpretation of the data, especially in parts of the superior longitudinal fasciculus.[48] Although we carried out a rigorous quality control at the edge level (eg, by varying the minimum required NOS per edge as well as applying a strict prevalence threshold), non-anatomical connections cannot be completely excluded and may have biased our results. Second, as the characteristics of brain networks are also influenced by the underlying brain parcellation scheme and applied preprocessing steps, our findings might be specific on the processing pipeline used, even though we have followed the current standards in the field. Furthermore, given the high density of the nodes, the resolution of the underlying DWI data is relatively low and may not adequately capture more complex fiber configurations. Third, in contrast to standard methods, some white matter regions that are often affected in neuropsychiatric disorders were not included in our analysis. Specifically, we considered only fibers connecting the atlas-defined (sub)-cortical brain regions. Therefore, fibers projecting to the brainstem, cerebellum, or spinal cord could not be examined, which may also (partially) explain why we did not detect areas with smaller FA in patients (cf Meneguzzo *et al.*[6]). Fourth, as in many other studies including those in severely ill patients, factors such as ventricular enlargement and head motion or hydration status might have biased our results. However,

there was no group difference for motion parameters (and all analysis were controlled for motion), and the young acAN group had a normal urine specific gravity (and urine specific gravity was not related to the network components). To account for partial volume effects, we performed several subanalyses such as controlling on the edge level for ventricular size, as well as using an adapted pre-processing procedure to correct for free water. Based on these subanalyses, we had to conclude that our finding based on NOS are not stable and may have been false-positive results. Furthermore, using the current graph theoretic approach, the group comparison of connectivity does not rely on registration of the native diffusion data to a common template, which might reduce a potential group bias due to registration inaccuracies, caused, for example, by ventricular enlargement. However, the labeling procedure of FreeSurfer is internally guided by a registration to the adult MNI305 template, which might represent a bias in our predominantly adolescent sample. Fifth, although our sample was thoroughly age matched (and although we conducted additional subanalysis in an exclusively adolescent sample), developmental effects and pubertal maturation effects[3] on network configurations cannot be ruled out entirely. Future studies may benefit from an adjustment for pubertal stage. Finally, the cross-sectional design of our study does not allow us to disentangle trait markers from possible state effects related to the severe undernutrition in acAN patients. To clarify whether aberrant WM network architecture is a consequence or a potential precursor of pathologic eating behavior, future longitudinal studies are needed.

The current study, which is the largest DWI study in AN to date, revealed evidence for altered WM network architecture in young acAN patients. The study design allowed us to control for metabolic state and hydration status.[3,49] Using an agnostic whole-brain approach, we identified a pattern of increased diffusion directionality that might indicate altered connectivity and possibly even increased efficiency of neural conduction among a number of brain regions. These implicated pathways (in particular, subnetworks involved in cognitive control and bodily awareness, processing of self-referential information, and interoceptive attention) have been associated with AN in several previous task-based fMRI studies and are also compatible with network analysis approaches from resting state functional connectivity dataset.[26,46,50] Taken together, these findings provide new insight into the neurobiology underlying this disorder by delivering evidence for an "altered network architecture" perspective.

Accepted April 30, 2021.

Messrs. Geisler, Bahnsen, Doose, Drs. King and Bernardoni, and Prof. Dr. Ehrlich are with the Division of Psychological and Social Medicine and Developmental Neurosciences, Faculty of Medicine, Technische Universität Dresden, Dresden, Germany. Prof. Dr. Ehrlich is with the Eating Disorder Treatment and Research Center, Faculty of Medicine, Technische Universität Dresden, Dresden, Germany. Mr. Müller and Dr. Marxen are with the Neuroimaging Center, Technische Universität Dresden, Dresden, Germany. Prof. Dr. Roessner is with the Child and Adolescent Psychiatry, University Hospital C. G. Carus, Technische Universität Dresden, Dresden, Germany. Prof. Dr. van den Heuvel is with the Connectome Lab, Center for Neurogenomics and Cognitive Research, Amsterdam Neuroscience, Vrije Universiteit Amsterdam, Amsterdam, The Netherlands.

This work was supported by the Deutsche Forschungsgemeinschaft (EH 367/5-1, EH 367/7-1, SFB 940/2), the Swiss Anorexia Nervosa Foundation, the Marga und Walter Boll-Stiftung, and the B. Braun-Stiftung.

Author Contributions
Conceptualization: Geisler, van den Heuvel, Ehrlich
Data curation: Geisler, Bernardoni, Doose, Müller
Formal analysis: Geisler, Bernardoni
Funding acquisition: Ehrlich
Investigation: Geisler, King, Bahnsen, Bernardoni, Doose
Methodology: Müller, van den Heuvel, Ehrlich
Project administration: King, Ehrlich
Resources: Müller, Marxen, Roessner, van den Heuvel, Ehrlich
Software: Geisler, Bernardoni, van den Heuvel
Supervision: van den Heuvel, Ehrlich
Validation: van den Heuvel, Ehrlich
Visualization: Geisler
Writing original draft: Geisler, Ehrlich
Writing review and editing: Geisler, King, Bahnsen, Bernardoni, Doose, Müller, Marxen, Roessner, van den Heuvel, Ehrlich

The authors would like to express their gratitude to all associated research assistants for their help with participant recruitment and data collection and thank all participants for their time and cooperation. The authors thank the Center for Information Services and High Performance Computing (ZIH) at Technische Universität Dresden for generous allocations of computer time.

Disclosure: Prof. Dr. Roessner has received payment for consulting and writing activities from Eli Lilly and Co., Novartis, and Shire Pharmaceuticals/Takeda, lecture honoraria from Eli Lilly and Co., Novartis, Shire Pharmaceuticals/Takeda, and Medice Pharma, and support for research from Shire Pharmaceuticals/Takeda and Novartis. He has carried out (and is currently carrying out) clinical trials in cooperation with Novartis, Shire Pharmaceuticals/Takeda, Servier, and Otsuka. He has reported no financial relationship with the organizations that sponsored the research. Drs. King, Bernardoni, Marxen, Prof. Drs. van den Heuvel and Ehrlich, and Messrs. Geisler, Bahnsen, Doose, and Müller have reported no biomedical financial interests or potential conflicts of interest.

Correspondence to Stefan Ehrlich, MD, PhD, Division of Psychological and Social Medicine and Developmental Neurosciences, Faculty of Medicine, Technische Universität Dresden, Fetscherstraße 74, 01307 Dresden, Germany; e-mail: transden.lab@uniklinikum-dresden.de

0890-8567/$36.00/

https://doi.org/10.1016/j.jaac.2021.04.019

REFERENCES

1. Bernardoni F, King JA, Geisler D, *et al*. Weight restoration therapy rapidly reverses cortical thinning in anorexia nervosa: a longitudinal study. NeuroImage. 2016;130:214-222. https://doi.org/10.1016/j.neuroimage.2016.02.003.

2. Kaufmann L-K, Hänggi J, Jäncke L, *et al*. Age influences structural brain restoration during weight gain therapy in anorexia nervosa. Transl Psychiatry. 2020;10:126. https://doi.org/10.1038/s41398-020-0809-7.

3. King JA, Frank GKW, Thompson PM, Ehrlich S. Structural neuroimaging of anorexia nervosa: future directions in the quest for mechanisms underlying dynamic alterations. Biol Psychiatry. 2018;83:224-234. https://doi.org/10/gcrq4h.
4. von Schwanenflug N, Muller DK, King JA, *et al*. Dynamic changes in white matter microstructure in anorexia nervosa: findings from a longitudinal study. Psychol Med. 2019;49:1555-1564. https://doi.org/10/gd5bg4.
5. Gaudio S, Carducci F, Piervincenzi C, Olivo G, Schiöth HB. Altered thalamo–cortical and occipital–parietal– temporal–frontal white matter connections in patients with anorexia and bulimia nervosa: a systematic review of diffusion tensor imaging studies. J Psychiatry Neurosci JPN. 2019;44:324-339. https://doi.org/10.1503/jpn.180121.
6. Meneguzzo P, Collantoni E, Solmi M, Tenconi E, Favaro A. Anorexia nervosa and diffusion weighted imaging: an open methodological question raised by a systematic review and a fractional anisotropy anatomical likelihood estimation meta-analysis. Int J Eat Disord. 2019;52:1237-1250. https://doi.org/10.1002/eat.23160.
7. Zhang S, Wang W, Su X, *et al*. White matter abnormalities in anorexia nervosa: psychoradiologic evidence from meta-analysis of diffusion tensor imaging studies using tract based spatial statistics. Front Neurosci. 2020;14:159. https://doi.org/10.3389/fnins.2020.00159.
8. Wakana S, Caprihan A, Panzenboeck MM, *et al*. Reproducibility of quantitative tractography methods applied to cerebral white matter. NeuroImage. 2007;36:630-644. https://doi.org/10.1016/j.neuroimage.2007.02.049.
9. Hayes DJ, Lipsman N, Chen DQ, *et al*. Subcallosal cingulate connectivity in anorexia nervosa patients differs from healthy controls: a multi-tensor tractography study. Brain Stimulat. 2015;8:758-768. https://doi.org/10.1016/j.brs.2015.03.005.
10. Travis KE, Golden NH, Feldman HM, *et al*. Abnormal white matter properties in adolescent girls with anorexia nervosa. NeuroImage Clin. 2015;9:648-659. https://doi.org/10.1016/j.nicl.2015.10.008.
11. Cha J, Ide JS, Bowman FD, Simpson HB, Posner J, Steinglass JE. Abnormal reward circuitry in anorexia nervosa: a longitudinal, multimodal MRI study. Hum Brain Mapp. 2016;37:3835-3846. https://doi.org/10.1002/hbm.23279.
12. Frank GKW, Shott ME, Riederer J, Pryor TL. Altered structural and effective connectivity in anorexia and bulimia nervosa in circuits that regulate energy and reward homeostasis. Transl Psychiatry. 2016;6:e932. https://doi.org/10.1038/tp.2016.199.
13. Pfuhl G, King JA, Geisler D, *et al*. Preserved white matter microstructure in young patients with anorexia nervosa? Hum Brain Mapp. 2016;37:4069-4083. https://doi.org/10.1002/hbm.23296.
14. Shott ME, Pryor TL, Yang TT, Frank GKW. Greater insula white matter fiber connectivity in women recovered from anorexia nervosa. Neuropsychopharmacology. 2016;41:498-507. https://doi.org/10.1038/npp.2015.172.
15. Fornito A, Bullmore ET, Zalesky A. Opportunities and challenges for psychiatry in the connectomic era. Biol Psychiatry Cogn Neurosci Neuroimaging. 2017;2:9-19. https://doi.org/10.1016/j.bpsc.2016.08.003.
16. Zalesky A, Fornito A, Bullmore ET. Network-based statistic: identifying differences in brain networks. NeuroImage. 2010;53:1197-1207. https://doi.org/10.1016/j.neuroimage.2010.06.041.
17. Zalesky A, Fornito A, Seal ML, *et al*. Disrupted axonal fiber connectivity in schizophrenia. Biol Psychiatry. 2011;69:80-89. https://doi.org/10.1016/j.biopsych.2010.08.022.
18. Tymofiyeva O, Connolly CG, Ho TC, *et al*. DTI-based connectome analysis of adolescents with major depressive disorder reveals hypoconnectivity of the right caudate. J Affect Disord. 2017;207:18-25. https://doi.org/10.1016/j.jad.2016.09.013.
19. Cammoun L, Gigandet X, Meskaldji D, *et al*. Mapping the human connectome at multiple scales with diffusion spectrum MRI. J Neurosci Methods. 2012;203:386-397. doi:10/fvcbh6.
20. Takao H, Hayashi N, Inano S, Ohtomo K. Effect of head size on diffusion tensor imaging. NeuroImage. 2011;57:958-967. https://doi.org/10/fxf5zx.
21. Kaufmann L-K, Baur V, Hänggi J, *et al*. Fornix under water? Ventricular enlargement biases forniceal diffusion magnetic resonance imaging indices in anorexia nervosa. Biol Psychiatry Cogn Neurosci Neuroimaging. 2017;2:430-437. https://doi.org/10.1016/j.bpsc.2017.03.014.
22. van den Heuvel MP, Mandl RCW, Stam CJ, Kahn RS, Hulshoff Pol HE. Aberrant frontal and temporal complex network structure in schizophrenia: a graph theoretical analysis. J Neurosci Off J Soc Neurosci. 2010;30:15915-15926. https://doi.org/10.1523/JNEUROSCI.2874-10.2010.
23. Mori S, Crain BJ, Chacko VP, van Zijl PC. Three-dimensional tracking of axonal projections in the brain by magnetic resonance imaging. Ann Neurol. 1999;45:265-269. https://doi.org/10.1002/1531-8249(199902)45. 2<265::aid-ana21>3.0.co;2-3.
24. Hagmann P, Sporns O, Madan N, *et al*. White matter maturation reshapes structural connectivity in the late developing human brain. Proc Natl Acad Sci U S A. 2010;107:19067-19072. https://doi.org/10.1073/pnas.1009073107.
25. de Reus MA, van den Heuvel MP. Estimating false positives and negatives in brain networks. NeuroImage. 2013;70:402-409. https://doi.org/10.1016/j.neuroimage.2012.12.066.
26. Ehrlich S, Lord AR, Geisler D, *et al*. Reduced functional connectivity in the thalamo-insular subnetwork in patients with acute anorexia nervosa. Hum Brain Mapp. 2015;36:1772-1781. https://doi.org/10.1002/hbm.22736.
27. Geisler D, Borchardt V, Boehm I, *et al*. Altered global brain network topology as a trait marker in patients with anorexia nervosa. Psychol Med. 2020;50:107-115. https://doi.org/10.1017/S0033291718004002.
28. Weninger L, Koppers S, Na C-H, Juetten K, Merhof D. Free-water correction in diffusion mri: a reliable and robust learning approach. In: Bonet-Carne E, Hutter J, Palombo M, Pizzolato M, Sepehrband F, Zhang F, eds. Computational Diffusion MRI. Mathematics and Visualization. New York: Springer International Publishing; 2020:91-99. https://doi.org/10.1007/978-3-030-52893-5 8.
29. Frank GKW, Shott ME, Hagman JO, Yang TT. Localized brain volume and white matter integrity alterations in adolescent anorexia nervosa. J Am Acad Child Adolesc Psychiatry. 2013;52:1066-1075.e5. https://doi.org/10.1016/j.jaac.2013.07.007.
30. Vogel K, Timmers I, Kumar V, *et al*. White matter microstructural changes in adolescent anorexia nervosa including an exploratory longitudinal study. NeuroImage Clin. 2016;11:614-621. https://doi.org/10.1016/j.nicl.2016.04.002.
31. Feldman HM, Yeatman JD, Lee ES, Barde LHF, Gaman-Bean S. Diffusion tensor imaging: a review for pediatric researchers and clinicians. J Dev Behav Pediatr JDBP. 2010;31:346-356. https://doi.org/10.1097/DBP.0b013e3181dcaa8b.
32. Keller TA, Just MA. Altering cortical connectivity: remediation-induced changes in the white matter of poor readers. Neuron. 2009;64:624-631. https://doi.org/10.1016/j.neuron.2009.10.018.
33. Seitz J, Herpertz-Dahlmann B, Konrad K. Brain morphological changes in adolescent and adult patients with anorexia nervosa. *J Neural Transm (Vienna)*. 2016;123:949–959. https://doi.org/10/f8wvrm
34. Kazlouski D, Rollin MDH, Tregellas J, *et al*. Altered fimbria-fornix white matter integrity in anorexia nervosa predicts harm avoidance. Psychiatry Res. 2011;192:109-116. https://doi.org/10.1016/j.pscychresns.2010.12.006.
35. Zastrow A, Kaiser S, Stippich C, *et al*. Neural correlates of impaired cognitive-behavioral flexibility in anorexia nervosa. Am J Psychiatry. 2009;166:608-616. https://doi.org/10.1176/appi.ajp.2008.08050775.
36. King JA, Korb FM, Vettermann R, Ritschel F, Egner T, Ehrlich S. Cognitive overcontrol as a trait marker in anorexia nervosa? Aberrant task- and response-set switching in remitted patients. J Abnorm Psychol. 2019;128:806-812. https://doi.org/10.1037/abn0000476.
37. Gallivan JP, Goodale MA. The dorsal "action" pathway. Handb Clin Neurol. 2018;151:449-466. https://doi.org/10.1016/B978-0-444-63622-5.00023-1.
38. Zhang S, Li CR. Functional connectivity mapping of the human precuneus by resting state fMRI. NeuroImage. 2012;59:3548-3562. https://doi.org/10.1016/j.neuroimage.2011.11.023.
39. Herbet G, Lemaitre A-L, Moritz-Gasser S, Cochereau J, Duffau H. The antero-dorsal precuneal cortex supports specific aspects of bodily awareness. Brain J Neurol. 2019;142:2207-2214. https://doi.org/10.1093/brain/awz179.
40. Li W, Lai TM, Bohon C, *et al*. Anorexia nervosa and body dysmorphic disorder are associated with abnormalities in processing visual information. Psychol Med. 2015;45:2111-2122. https://doi.org/10.1017/S0033291715000045.
41. Watson HJ, Yilmaz Z, Thornton LM, *et al*. Genome-wide association study identifies eight risk loci and implicates metabo-psychiatric origins for anorexia nervosa. Nat Genet. 2019;51:1207-1214. https://doi.org/10.1038/s41588-019-0439-2.
42. Wagner G, Koch K, Schachtzabel C, *et al*. Self-referential processing influences functional activation during cognitive control: an fMRI study. Soc Cogn Affect Neurosci. 2013;8:828-837. https://doi.org/10.1093/scan/nss074.
43. McAdams CJ, Krawczyk DC. Who am I? How do I look? Neural differences in self-identity in anorexia nervosa. Soc Cogn Affect Neurosci. 2014;9:12-21. https://doi.org/10.1093/scan/nss093.
44. Doose A, King JA, Bernardoni F, *et al*. Strengthened default mode network activation during delay discounting in adolescents with anorexia nervosa after partial weight restoration: a longitudinal fMRI study. J Clin Med. 2020;9. https://doi.org/10.3390/jcm9040900.
45. Kashkouli Nejad K, Sugiura M, Nozawa T, *et al*. Supramarginal activity in interoceptive attention tasks. Neurosci Lett. 2015;589:42-46. https://doi.org/10.1016/j.neulet.2015.01.031.
46. Geisler D, Borchardt V, Lord AR, *et al*. Abnormal functional global and local brain connectivity in female patients with anorexia nervosa. J Psychiatry Neurosci JPN. 2016;41:6-15. https://doi.org/10.1503/jpn.140310.
47. Gaudio S, Olivo G, Beomonte Zobel B, Schiöth HB. Altered cerebellar–insular–parietal–cingular subnetwork in adolescents in the earliest stages of anorexia nervosa: a network–based statistic analysis. Transl Psychiatry. 2018;8:1-10. https://doi.org/10.1038/s41398-018-0173-z.
48. Alexander AL, Lee JE, Lazar M, Field AS. Diffusion tensor imaging of the brain. Neurother J Am Soc Exp Neurother. 2007;4:316-329. https://doi.org/10.1016/j.nurt.2007.05.011.
49. Frank GKW, Favaro A, Marsh R, Ehrlich S, Lawson EA. Toward valid and reliable brain imaging results in eating disorders. Int J Eat Disord. 2018;51:250-261. https://doi.org/10.1002/eat.22829.
50. Boehm I, Geisler D, King JA, *et al*. Increased resting state functional connectivity in the fronto-parietal and default mode network in anorexia nervosa. Front Behav Neurosci. 2014;8:346. https://doi.org/10.3389/fnbeh.2014.00346.